THE PROTO-ONCOGENE FYN INHIBITS THE ANTI-GLIOBLASTOMA IMMUNE RESPONSE

Andrea Comba[1,2], Patrick J Dunn[1,2], Anna E Argento[1,2], Padma Kadiyala[1,2], Maria Ventosa[1,2], Daniel B Zamler[1,2], Priti Patel[1,2], Lili Zhao[3], Felipe J Nunez[1,2], Maria G Castro[1,2], Pedro R. Lowenstein[1,2,*]

[1]Department of Neurosurgery, University of Michigan Medical School, Ann Arbor, MI 48109

[2]Department of Cell and Developmental Biology, University of Michigan Medical School, Ann Arbor, MI 48109

[3]Department of Biostatistics, University of Michigan Medical School, Ann Arbor, MI 48109

[*]Corresponding Author: Pedro R Lowenstein. MSRB II, Room 4570, Department of Neurosurgery University of Michigan School of Medicine, 1150 West Medical Center Drive, Ann Arbor, MI 48109-5689. Phone (office) 734-764-0851. Email: pedrol@umich.edu

ABSTRACT

In vivo genetic knockdown of the proto-oncogene Fyn in immunocompetent mouse glioma models significantly extended survival by 25%-77%. GSEA analysis of DE genes revealed a highly significant enrichment of gene ontologies related to immune function such as STAT-1 regulated cell differentiation, IFNγ signaling, T cell activation, and NK cytotoxicity. At the gene level, STAT1, and downstream genes IFNγ, IRF1, NLRC5, CIITA, TAP1, CXCL9, CCL5, H2-Q4 and H2-DMa were upregulated in Fyn-knockdown tumors. These data indicate that Fyn downregulation increases expression of STAT1, a major coordinator of immune responses. These data predict that knockdown of Fyn should only extend survival in immunocompetent mice. Indeed, in immune-deficient NSG mice the effect of Fyn-knockdown was minimal. Our data indicate that Fyn exerts its main pro-tumoral activity by downregulating the anti-glioma immune response. We propose the specific inhibition of Fyn as a novel therapeutic target in gliomas.

INTRODUCTION

Glioblastomas (GBM) are the most frequent and aggressive primary tumors of the central nervous system [1]. Molecular characterization of human gliomas and genetically engineered mouse models allow to study the role of individual genes in glioma development, growth, and overall malignity [2]. Cellular transformation and increased glioma malignity is in large part a consequence of increased activity of constitutively active/mutated growth factor receptors (EGFR, PDGFR, HGF/MET, RTK/RAS/PI3K), and/or their downstream transduction pathways [3]. In addition, tumors can increase their aggressiveness by downregulating innate and adaptive immune responses in the tumor microenvironment [4,5]. This changes the proliferation, invasion, and survival of glioma cells. A remaining experimental challenge is to discover the molecules involved in the transduction of these oncogenic signals. Whether these signaling pathways also induce changes in the tumor microenvironment remains unknown.

To identify signaling pathways that modulate driver gene activity in glioma tumor progression and malignancy we utilized RNA-sequencing and compared gene expression in highly malignant stem cells derived from NPA (Nras, shp53, shATRx and IDH-Wild Type) gliomas with glioma stem cells derived from less aggressive tumors NPAI (Nras, shp53, shATRx IDH1^{R132H}). The set of differentially expressed (DE) genes was mined using bioinformatics and network analysis. The result was a heterogeneous and non-random network, i.e., the graph of number of gene nodes vs. the degree of each node obeys a power law. This predicts the existence of hubs, gene nodes with high connectivity. Fyn tyrosine kinase was one of the four most highly connected hubs. We tested the hypothesis that Fyn is a significant transducer of glioma growth and malignancy.

Fyn tyrosine kinase is a non-receptor membrane protein member of the Src family of tyrosine kinases [6]. In normal physiology Fyn regulates neuronal development and signaling in T and B-cells [7-11]. In oncology, Fyn has been described as a proto-oncogene in pancreas, prostate, breast, and hematological cancers. It has been shown that the oncogenic pathways of EGFR, PDGFR, HGF/MET or RTK/RAS/PI3K signal through Fyn to increase invasion and reduce cell death [12-14].

In gliomas Fyn has been associated with increased cell migration and proliferation in *in vitro* studies, but has provided contradictory results when tested *in vivo* [12,15,16]. *In vivo* studies using a glioma orthotopic xenograft model for Fyn knockdown showed no difference in survival compared to control [15]. In glioma, studies inhibiting SFK with the non-specific inhibitors Saracatinib, Dasatinib or PP2 decreased cell proliferation, migration and invasion [12,17-19] *in* vitro, and tumor growth in immune-suppressed animals. Studies in immune-suppressed animals, necessary when using PDX models, are nevertheless limited, as they do not allow us to assess potential effects on the immune system.

Network analysis identified Fyn as a gene with potentially important regulatory functions. To test this hypothesis, we analyzed the behavior of glioma cells transduced with shRNA-Fyn *in* vitro, and in immune-competent, and immune-deficient mice. *In vitro* we detected a reduction in proliferation and migration. *In vivo*, selective downregulation of Fyn increased survival of tumor bearing m and decreased tumor growth and malignancy. Increased survival of shRNA-Fyn transduced gliomas is lost when such tumors are implanted into immunesuppressed mice.

In summary, data from our transcriptomic and network analysis, the genetic downregulation of Fyn, and experiments in immune-competent v. immune-deficient mice strongly suggests that an important contribution of the pro-tumoral effect of Fyn might be exerted through inhibition of anti-glioma immune responses. We propose that Fyn is a novel target to inhibit tumor progression, increase the sensitivity of gliomas to immune attack, and could be exploited for the personalized treatment of glioma patients.

RESULTS

Network analysis of differentially expressed genes in mouse and human glioma of high vs. low malignant behavior. Identification of Fyn as a potential regulator of glioma progression.

Differential expression (DE) of genes in mouse and human glioma primary stem cells was analyzed to identify genes that regulate glioblastoma progression. We compared phenotypically more aggressive NPA-neurospheres (Nras, shp53, shATRx and IDH-Wild Type) with less malignant NPAI-neurospheres (Nras, shp53, shATRx $IDH1^{R132H}$) [20]. The network of DE genes revealed the existence of a heterogeneous, non-random, network whose node degree distribution (number of nodes v. node degree) obeys a power law (correlation=0.935; r^2=0.792). These characteristics predict the existence of hubs, which are highly connected nodes that play essential roles in network function. We identified Fyn to be one of the most highly connected nodes (Degree: 63; 4^{th} node from top node) in the network **(Fig. 1a).**

To analyze the role of Fyn in human glioma derived stem cells, we extended our network analysis to two human glioma stem cells of differential aggressiveness [21]. We compared DE genes of MGG8-adherent cells, a less aggressive cell type which does not form tumors in NSG mice, with MGG8-Spheres cells, a more aggressive cell type that does form tumors in NSG mice. This analysis also revealed Fyn to be one of the most connected nodes in the network (Degree: 47; 7^{th} node from top node) **(Fig. 1c)**. **Fig. (1b)** and **(1d)** display the set of nodes that are first neighbors of Fyn. Detailed information of genes present in each of networks is shown in **Supplementary Table 1 a-b**.

We then performed a network functional enrichment analysis (GSEA) to determine the Gene Ontologies (GO)/Biological Process enriched in the networks using the Reactome App of Cytoscape. We identified the most relevant GO Biological Processes involving Fyn for NPA vs NPAI cells and MGG8-Sphere vs MGG8-Adherent cells using a cutoff of FDR<0.2, p-value<0.05

(Supplementary Table 2a-d). GO term analysis from both networks identified 14 shared GO Biological Processes involving Fyn **(Fig. 1e)**. The full list of GO terms are shown in **Supplementary, Tables 2a-b** and **2c-d** respectively. These GO terms represent functions by which Fyn is thought to exerts its effects. To establish whether Fyn levels correlate with glioma malignancy, we used RNA-Sequencing and Microarray data from the Gliovis (http://gliovis.bioinfo.cnio.es) database. Fyn mRNA expression levels were higher in different types of human gliomas (i.e. Unknown, Mixed glioma, Oligodendroglioma, Astrocytoma and Glioblastoma) when compared to normal brain tissue according to Rembrandt, TCGA, and Gravendeel databases **(Fig. 2a-c)**. Western blot analysis of mouse and human glioma stem cells revealed that Fyn protein levels correlate positively with tumor malignancy **(Fig. 2d).**

Saracatinib, a Src family kinase inhibitor, impairs cell viability and migration in correlation with glioma cell malignancy.

Due to Fyn being a hub in our network analysis and a potential regulator of glioma progression, we sought to determine whether inhibiting Fyn activity has an effect on the *in vitro* proliferation and migration of glioma cells. Western blot (WB) analysis shows that the Src family kinase (SFK) inhibitor, Saracatinib, inhibited SFK activation. A low dose of 0.5 μM Saracatinib inhibited the SFK activation site (Y416 phosphorylation) in all glioma cells. Moreover, Saracatinib significantly inhibited the phosphorylation of the inactive site Y530 of SFKs at 0.5 μM in NP cells, but higher doses of the inhibitor were required to achieve a similar decrease of Y530 phosphorylation in NPA, GL26 and NPAI cells. We observed that Fyn protein levels were unchanged due to the Saracatinib treatment in NP, NPA and GL26 cells. However, we observed that Fyn protein levels were upregulated in NPAI cells due to the Saracatinib treatment **(Fig. 3a)**. We also evaluated cell proliferation and cell migration in response to Saracatinib. Saracatinib significantly decreased cell viability in GL26, NP and NPA cells in a dose-dependent manner after 72 and 96 hours of treatment, but did not have an effect on NPAI cells (**Fig. 3b**). However, the Saracatinib DL50 was

at higher doses than doses shown to inhibit SFK–phosphorylation **(Fig. 3a).** Cell migration determined by Transwell migration assay, showed that Saracatinib significantly decreased migration of NP, NPA and GL26 cells in a dose dependent manner, but only had a less strong effect on the migration of NPAI cells (**Fig. 3c and 3d**). Using human glioma stem cells, we also demonstrated that Saracatinib decreased cell proliferation and migration in MGG8-spheres more effectively than MGG8-adherent cells **(Supplementary Fig. 1a and 1b**). These results suggest that the inhibition of SFK activity by Saracatinib treatment has a greater effect on cell migration than on proliferation. These experiments demonstrate the effects of SFK on the behavior of glioma stem cells. They do not allow us to pinpoint the individual effects of Fyn. To do so, we performed genetic knockdown of Fyn expression.

Genetic knockdown of Fyn reduces *in vitro* glioma cell proliferation and migration

To evaluate the effects of Fyn in glioma cells, we generated stable cell lines with Fyn knockdown using lentiviral vectors expressing shRNA against Fyn. We chose two mouse glioma cell types that are highly aggressive (NP, NPA) to achieve the Fyn knockdown. WB analysis in NP and NPA cells showed that two shRNAs (shFyn #1 and shFyn#2) decreased Fyn protein levels compared with the non-target (NT)-control vector **(Supplementary Fig. 2a-b)**. ShFyn #2 displayed a stronger knockdown for Fyn and was chosen for all studies described further. The level of phosphorylation of the SFK active site P-Y416 was decreased upon Fyn downregulation. Importantly Src expression was not reduced post Fyn knockdown, confirming the specificity of the shRNA-Fyn (**Supplementary Fig. 2a-b**). We evaluated the effect of Fyn knockdown on glioma cells' proliferation. We found that NPA and NP cells that were knocked for Fyn exhibited a significantly decreased cell proliferation compared their corresponding control cells (**Fig. 4a-b**). Transwell migration assays were performed to assess the effect of Fyn on glioma cell migration *in vitro*. The analysis showed that Fyn knockdown significantly decreased the ability of NP and NPA cells to migrate through the trans-well membrane in response to CXL12, EGF and FGF.

Migration of cells that were expressing shFyn #2 significantly decreased compared to cells that were expressing shFyn #1 (**Fig. 4c-d**). These results indicate that Fyn knockdown has a strong effect on cell proliferation and migration in glioma cells.

Knockdown of Fyn reduces tumor growth and prolongs survival in an intracranial mouse glioma model

To assess if knocking down Fyn has an effect on tumor development *in vivo*, we used an implantable syngeneic murine glioma model. Intracranial NP-NT or NP-shFyn tumors were established in immunocompetent mice. Median survival was significantly increased in animals harboring tumors with Fyn knockdown (MS: 34 days) compared with the NP- NT control group (MS: 27 days) (**Fig 4e**). Moreover, we analyzed the effect of Fyn *in vivo* through intracranial implantation of NPA-NT and NPA-shFyn cells. Survival analysis also demonstrated that tumors harboring the knockdown of Fyn had a significantly higher median survival (MS: 30 days) than the control group (MS: 20) (**Fig. 4g**).

Immunofluorescence analysis displayed the downregulation of Fyn expression levels in the NP-shFyn and NPA-shFyn tumor tissues compared with their corresponding controls (**Fig. 4f-h**). Moreover, we observed that tumor growth and development was decreased with Fyn downregulation. *In vivo* bioluminescence imaging and quantification of tumors at day 13 post tumor implantation showed that NP-Fyn knockdown tumors exhibited significantly lower bioluminescence signal (Photon/second) compared to the control group (**Fig. 4i**). Additionally, tumor size evaluation at necropsy showed a correlation with *in vivo* tumor bioluminescence analysis. NP-shFyn tumors had a smaller tumor size at 25 days than the control NP-NT tumors (**Fig. 4j**). Taken together, these results suggest that the individual downregulation of Fyn is able to decrease glioma growth and malignancy *in vivo*.

Fyn knockdown reduces tumor malignancy and prolongs the survival of mice harboring GEMM tumors

The above results suggest that Fyn is a potent gene involved in a pro-tumorigenic glioma phenotype. The Sleeping Beauty Transposon System GBM model (GEMM) was used to understand the function of Fyn in *de novo* tumors generated from the host brain progenitors cells[2]. We generated a Fyn-deficient genetically engineered mouse glioma model (**Fig. 5a-b**). We performed the cloning of two different shRNAs for Fyn into the PT2-GFP4 vector. We corroborated the efficacy of the shRNAs of Fyn by WB analysis (**Fig. 5c**). The shFyn-(b) was selected for the GEMM glioma generation. We generated tumors harboring different genotype combinations. We induced tumors by: (1) NRAS pathway activation in combination with shp53 (NP); (2) NRAS activation, shp53 and shFyn (NPF), (3) NRAS, shp53, and shATRX (NPA), (4) shp53, NRAS, shATRX and shFyn (NPAF), (5) shp53, NRAS and PDGFβ (NPD), (6) shp53, NRAS, PDGFβ and shFyn (NPDF) (**Fig. 5d**). We were able establish tumors with all the experimental groups. Downregulation of Fyn increased median survival (MS) compared with their control groups (**Fig. 6-a-c**). The downregulation of Fyn in the NPF group displayed an increased MS of 131 days compared with 94 days in the NP control group (**Fig. 6a**). The experimental group with knockdown of Fyn in the context of ATRX loss (NPAF) exhibited an increased survival (MS: 142 days) compared with the NPA control (MS: 80 days), (**Fig. 6b**). In the third experimental group, Fyn knockdown plus PDGFβ ligand upregulation (NPDF), also displayed an increased MS of 108 days compared with the NPD control group (MS: 69 days) (**Fig. 6c**). We evaluated the expression of Fyn in tumor tissue by immunofluorescence. We corroborated the downregulation of Fyn protein in all experimental groups as shown in **Fig. 6d, 6e** and **6f** respectively. In addition, *in vivo* bioluminescence imaging signal intensity was reduced in Fyn knockdown groups, indicating slower tumor development. Further, we analyzed tumor malignancy by histopathology of tumors. There was no evidence of significant differences in glioma malignant pathological markers. Both Fyn-knockdown and control tumors contained pseudo-palisades, necrotic areas, hemorrhages,

micro-vascular proliferation, giant cells, a mesenchymal sarcomatous component, and small cells (**Fig. 6g, h, i**). Changes in individual pathology parameters are detailed in **Fig. 6j**. We further evaluated cellular proliferation of the tumor by immunostaining of P-H3-Serine-10. Quantification demonstrated a significant decrease in the ratio of P-H3-S10 cells per total cells in Fyn knockdown groups (**Fig. 6k-m**). These data demonstrate that Fyn downregulation increases animal survival by decreasing tumor development and proliferation.

RNA Sequencing and bioinformatics analysis indicates immune activation in Fyn knockdown as a mechanism in glioma growth and malignancy modulation

RNA Sequencing and bioinformatics analysis was used to uncover the mechanism by which Fyn knockdown leads to the inhibition of tumor growth and progression. These studies were performed on NP and NP-shFyn genetically engineered gliomas. RNA-seq analysis of NP-shFyn tumors versus NP tumors revealed a group of 567 differentially expressed genes. From the total DE genes, 226 genes were upregulated and 341 genes were downregulated (**Fig. 7a**). Using network analysis (i.e., Cytoscape) we analyzed the functional interaction of the DE genes resulting from Fyn knockdown. Up-regulated genes (red border node) and down-regulated genes (green border node) are shown in the network (**Fig. 7b**). We found that the following pathways were impacted in the network: Extracellular matrix organization, β1 integrin cell surface interactions, signaling by PDGF, ECM-receptor interaction, signaling by interleukins and IFNγ among others (**Supplementary Fig. 3a and Supplementary Table 3**).

In addition, the analysis of the network interactions revealed STAT1 gene (Degree: 20) as the highest connected node in the network followed by ITGA2 (Degree:15), ITGA3 (Degree: 15), ITGA9 (Degree: 14), GNA14 (Degree:14), ITGBLI (Degree: 13), ITGAL (Degree: 11) and CAMK2A (Degree: 11) (**Fig. 7b**). These genes represent the leading regulators of the network. These genes are part of different functional modules, formed by highly interacting group of genes in the network. We analyzed the functional enrichment pathways impacted in each module (**Fig.**

7c). We found that the ITGA module (M0) regulated extracellular matrix organization, ECM receptor interactions, and integrin signaling. The STAT1 module (M1) regulated immune functions including the JAK-STAT pathways, cell differentiation of Th1, Th2 and Th17, IFNγ signaling, T cell activation and NK cell mediated cytotoxicity. The GNA14 module (M2) mainly modulated the Wnt signaling pathways and the cadherin signaling pathways. The CAMK2A module (M4) was involved in cAMP signaling, EGFR and PDGF signaling, and RAF/MAP kinase cascade. These results show that the immune pathways modulated by STAT-1 are the most enriched in the network **(Fig. 7c)**.

The functional associated Gene Ontologies (GO) by gene set enrichment analysis (GSEA) suggest that Fyn knockdown induces a strong activation of immune response in our GEMM (**Fig. 7d**). The analysis showed that 315 / 709 GO terms were upregulated in NPF gliomas and 24 GO terms were significant at FDR < 0.1 and nominal p-value < 0.05 (**Fig 4d**). However, there were no downregulated GO terms in NPF that were significantly enriched at a FDR <0.1 and p-value <0.05. At a less stringent FDR<1 and p-value <0.05, 15 downregulated GO terms were significantly enriched in the NPF gliomas **(Supplementary Fig 3b).** Detailed enrichment results are shown (**Supplementary Table 4a and 4b)**. The analysis of the upregulated GO terms indicated that the GO: “Cell Chemotaxis” (FDR: 5.94E-04 and NES: 2.68) and GO: “Immune response” (FDR: 0.016 and NES: 2.29) are some of the most significantly enriched biological functions elicited by Fyn downregulation (**Fig. 7e**). The analysis also included significant immune related GO terms such as: “Leukocyte Chemotaxis”, “Innate Immune Response”, “Response to Interferon Gamma” and “Adaptive Immune Response (**Fig. 7e**)”. These GO terms are involved in the mechanism by which Fyn knockdown decreases glioma malignancy. Details of the selected GO terms are shown in **Supplementary Table 5a-f**. The enrichment plots with the Running Enrichment Score and the positions of genes in the selected GO terms are shown in **Fig. 7e** and **Supplementary Fig. 3c**.

The mRNA expression analysis of NP tumors compared with Fyn knockdown NPF tumors for the GO terms, “Immune response” and “Cell Chemotaxis”, indicated a group of highlighted DE genes. The GO Immune response exhibited significant increased levels of genes, such as: STAT1 (q-value=0.04), ITGAL (q-value=0.006), CIITA (q-value=0.004), IRF1 (q-value=0.01), IRF8 (q-value=0.004) NLRC5 (q-value= 0.004) and TAP1 (q-value= 0.009). (**Fig. 8a, left panel**). The GO: “Cell Chemotaxis” include the following differentially expressed genes: ITGA9 (q-value=0.004), IFNG (q-value=0.004), CXCL9 (q-value=0.004), CCL1 (q-value= 0.004), CCL5 (q-value= 0.04) and PDGFRB (q-value=0.02) **(Fig. 8a, right panel)**. All DE gene levels of the respective GO are listed in the heat map graphs (**Fig 8a**). We next explored to see if Fyn affects the anti-tumor immune system response *in vivo*.

Tumors were generated through intracranial implantations of NPA-Empty and NPA-shFyn cells in immune-compromised mice (NSG) and in immune-competent mice (C57BL/6) (**Fig. 8b**). We observed that Fyn knockdown tumors had a significantly increased MS (24 vs 34 dpi) in immune-competent mice than in immune-compromised mice when compared to the control tumors. We also observed a small increase in MS (22 vs 24 dpi) of NSG mice bearing NPA-shFyn tumors compared to mice bearing NPA-Empty tumors (**Fig. 8b**).

We next studied the impact of Fyn downregulation on STAT1 signaling and anti-tumor immune response. We used the cBioPortal cancer genomics correlation analysis to compare gene expression and network structure of our GEMM, with the human glioma TCGA gene expression data. The analysis indicated that decreased levels of Fyn in the GEMM and human gliomas were inversely correlated with STAT1 levels and the functional related genes CXCL9, NLRC5, CIITA, IL12RB1, CD3E, IL2R, IRF1, IRF8, BATF2, SH2D1A and SLAMF7 (**Fig. 8c**). Taken together, these results suggest a strong effect of Fyn downregulation in the activation of the anti-tumor immune response through the modulation of the described pathways.

DISCUSSION

In this study we demonstrate that the knockdown of Fyn expression uncovers its capacity to downregulate the anti-glioma immune response. As a proto-oncogene Fyn's typical cell autonomous effects, such as changes in cell proliferation and migration, had been studied earlier, and were confirmed by us. The existence of non-cell autonomous effects of Fyn on the capacity of tumor cells to respond to the immune system, and on the activation of anti-glioma immune responses, were not previously suspected. We propose that most of the pro-glioma effects of Fyn are the result of its capacity to inhibit anti-tumor immune responses.

Fyn is a non-receptor tyrosine-protein kinase member of the Src family kinases with important roles in the immune system, the nervous system, and most recently, in cancer. In the CNS, it regulates axon guidance, cell proliferation, cell adhesion and cell migration during brain development [11,13,22,23]. In T cells Fyn induces cell-autonomous effects. It is expressed in T cells where it has important roles in the regulation of T cell effector functions [7,24,25]. For example, it activates antigen-specific naïve CD4 T cell responses, and its knockout impairs T cell activation[26]. Fyn also play a critical role propagating and amplifying T-cell antigen receptor (TCR) signaling[7].

The search for glioma driver genes has resulted from sequencing and mutation analysis of human tumors [27]. Important driver genes in glioblastoma are the epidermal growth factor receptor (EGFR), the platelet derived growth factor receptor (PDGFR), and MET, the receptor for the hepatocyte growth factor (HGF). Elucidating the transduction pathways involved in malignant transformation and tumor progression in glioma has not been yet achieved. It is likely that these genes are not necessarily mutated, as their transduction activity can change due to transcriptional or post-translational modifications in the absence of mutations. Fyn is mutated in in a very low percentage (0.1-0.4 %) of human gliomas [28,29].

In this study, we demonstrate the importance of studying comparative functional gene interaction networks of tumors of different malignity to identify key potential glioblastoma regulating oncogenic pathways and networks. Our findings from the network analysis of differentially

329 expressed genes of highly malignant versus less malignant glioma stem cells highlighted Fyn as
330 a highly connected node. This analysis suggested that Fyn is a central hub in the DE network and
331 a potential major regulator of glioma malignancy.
332 Furthermore, human glioblastoma expression analysis from the Rembrandt, TCGA and
333 Gravendeel databases [30], and data from Lu *et al* [12] demonstrate an increased expression of Fyn
334 in human gliomas. These studies correlate with our results of Fyn expression in mouse and human
335 glioma stem cells with diverse malignant capacity which show that Fyn is overexpressed in the
336 more malignant cells.
337 Previous studies of Fyn's role in different cancers [12,13,22,23,31] correlate with our findings, i.e., that
338 Fyn is involved in cell migration, cell proliferation, PIK3 and EGFR signaling, MAPK cascade
339 regulation, response to EGFR, MET, PDGF and TGF-beta. Non-autonomous effects of Fyn
340 expressed by cancer cells on the regulation of immune responses has not yet been described.
341 *In vitro* and *in vivo* studies [12,16-18] using pan Src family kinase inhibitors such as Saracatinib,
342 Dasatinib or PP2 suggested a role for Fyn in increasing cell proliferation, migration and tumor
343 growth and invasion in different cancers including gliomas. Our experiments showed that
344 Saracatinib decreased cell migration but only had a small effect on cell proliferation. These effects
345 were also positively correlated with glioma cells aggressiveness.
346 The non-specificity of available SFK inhibitors limits the ability to attribute specific effects to
347 individual kinases [32]. Attempts to discover selective Fyn inhibitors [33], have so far been
348 unsuccessful, thought there is currently a strong push for industry to find novel Fyn inhibitors,
349 particularly to treat Alzheimer's Disease. Thus, the genetic inhibition of Fyn remains the best
350 option to study its functions.
351 *In vitro* studies of Fyn effects on cell proliferation and migration, reported by Kan V. Lu et al [12] and
352 others [12,15,16,34] using siRNA to inhibit Fyn in human glioma cells obtained equivocal findings, with
353 positive [12,15,34] and also negative results [16] . In our experiments, selective genetic downregulation

of Fyn in glioma cells resulted in a significant decrease in the proliferation and migration of murine and human glioma stem cells.

Previous studies *in vivo*, have been inconclusive. Studies reported by Lewis-Tuffin and colleagues [15] using an implantable glioma model in immune-deficient mice demonstrated inhibitory effects for the SFK member Lyn, but failed to detect effects of Fyn, or others SFK members. However, our results indicate that Fyn is a significant regulator of glioma growth and malignancy *in vivo*. We demonstrated increases in survival and decreased tumor growth using immune-competent mice implanted with glioma stem cells genetically engineered with shRNA-Fyn, or using GEMMs with plasmids that encode genes to induce glioma as well as shRNA-Fyn.

The genetic analysis indicates that Fyn downregulation in tumor cells activates the anti-tumor immune response. The GSEA analysis discovered a group of immune related gene ontologies, such as “Innate immune response”, “Adaptive immune response”, “Response to IFNγ” and “Leukocyte chemotaxis” as some of the most enriched GO terms in our model, having highly significant q values. We thus propose a new mechanism by which Fyn knockdown in the glioma cells induces the activation of the tumor immune response. The central role of the immune system is supported by implantation of Fyn knockdown glioma cells in NSG immune-deficient mice. In immune-deficient mice, Fyn knockdown provided a very minor survival benefit, compared to the one obtained in immune-competent mice after implantation of murine glioma stem cells, or, following induction of GEMM incorporating shRNA-Fyn.

We also detected that the signal transducer and activator of transcription (STAT1) is overexpressed in Fyn downregulated tumors. In human glioma genomic expression, STAT-1 is also in opposite correlation with Fyn expression [35,36]. In addition, we verified that STAT-1 protein is overexpressed in the tumor cells when Fyn is knocked down. Moreover, the network interaction analysis shows that when Fyn is downregulated STAT1 is a central node with a principal role in immune system regulation. STAT1 is a cytoplasmic transcription factor activated by cytokines and

379 growth factor receptors [37]. Many others [38-41] have shown that STAT1 triggers pro-apoptotic and
380 anti-proliferative responses through increasing the anti-tumor immunity in different cancers.
381 STAT-1 activation and nuclear translocation is activated by IFNγ [42].
382 IFNγ is mainly produced by T cells and NK cells. It can induce a positive feedback in the STAT1
383 pathway that increases the immune response in the tumor microenvironment [38,41]. STAT-1
384 triggers the expression and activation of IRF-1, IRF8, NLRC5, CIITA, which induce the expression
385 of genes that participate in antigen presentation (i.e: TAP1, CXCL9, CCL1, H2-Q4 and H2-DMa,
386 H2-Aa, H2-Ab1) [39,41,43-45]. These genes, as well as other immune-related genes, were
387 overexpressed in our RNA-Seq analysis of Fyn knockdown glioma models. The GSEA analysis
388 confirms that these genes are part of the immune gene ontologies over-represented in our
389 models. As supported by the genetic and network analysis, we suggest that the effect of Fyn on
390 glioma survival is due to its modulation of both the anti-glioma immune response as well as the
391 capacity of tumor cells to respond to immune attack. For example, our data indicate that Fyn
392 regulates expression MHC Class I and II (H-2 antigens), as well as STAT1 signaling and changes
393 in IFNγ secretion. We conclude that the inhibition of Fyn expression causes an increase in the
394 anti-tumor immune response. We propose that this effect is responsible for the increased
395 longevity of animals bearing tumors with knocked down Fyn. Under pathological conditions we
396 propose that the main roles of Fyn's pro-tumoral activity are the combined effects on reducing
397 expression of pro-immunogenic genes in tumor cells, and indirectly, by causing an inhibition of
398 the anti-glioma immune response.
399 We propose that Fyn inhibition in tumor cells could be a novel therapeutic target in gliomas.
400 Furthermore, combination of Fyn inhibition with cancer immunotherapy as immune checkpoint
401 blockade (PDL1-PD1 inhibitors), IFNγ treatment, Ad-hCMV-TK and Ad-hCMV-Flt3L treatment
402 [5,42,46] are promising avenues to explore novel treatment for gliomas.
403
404

METHODS

Glioma cells and culture conditions. Primary mouse neurospheres glioma cells: Mouse neurospheres were derived from genetically engineered mouse models (GEMM) of gliomas generated in our lab using the Sleeping Beauty (SB) transposon system. These methods were previously described by us in detail in Koschmann et al., 2016, Wiesner *et al*, 2009. [2,47]. Glioma neurospheres exhibit the activation of the RTK/RAS/PI3K pathway, the knockdown of p53 and with or without another specific gene modification as described: NP (N-Ras and shp53), NPA (N-Ras, shp53 and shATRX), and NPAI (N-Ras-shp53-shATRX and mutant IDH^{R132H} expression) [2,20]. Mouse adherent glioma cells: The mouse glioma cell line GL26 was used and maintained as described in Supplementary Information. Human glioma stem cells: The human glioma derived stem cell MGG8 was obtained from Samuel Rabkin, Harvard University. All cells were maintained as described in Supplementary Information.

***In vitro* cell treatments.** Cells were treated with Saracatinib (AZD0530) a Src family pan inhibitor (Selleck Chemicals, Houston, TX) [18]. Saracatinib was diluted in absolute ethanol at an initial concentration of 50 mM. Cells were treated with increasing concentrations of Saracatinib for 48,72 or 96 hours as described for each experiment in detail, above. Treatment was performed to analyze glioma cell proliferation and migration.

***In vitro* cell viability assay.** Cell viability was analyzed using the CellTiter-Glo® Luminescent Assay (Promega Corp. Madison, WI, US) as recommended by the manufacturer. 1000 cells/well were plated in opaque-walled 96-well plates and cultured in 100 ul of their respective media. Cells were grown for up to 96 hrs to analyze cell proliferation. For Saracatinib treatment experiments, cells were treated with increased concentrations of Saracatinib (0.026, 0.06, 0.16, 0.4, 1, 2.5, 6.5, 16 uM) or the corresponding control vehicle (ethanol). After the desired period, cells were lysed by adding 100 ul of Cell Titer Glo reagent, mixed by pipetting, and incubated for 10 minutes at

room temperature. Luminescence was recorded using the Veritas™ Microplate Luminometer (Turner Biosystems, Inc). Cell viability at day zero was determined as a seeding control and used for normalization.

***In vitro* cell migration assay.** Transwell migration assays were utilized to determine cell migration *in vitro.* Transwell® polycarbonate membrane inserts (Corning Inc.) of 6.5 mm diameter and 8 um pore size were utilized for all assays. A suspension of 50,000 cells in 100 ul of NSC medium without growth factors was seeded on the top of the Transwell insert. The bottom well was filled with 600 ul of NSC media. The bottom well was supplemented with 50 nM CLX12 in assays using attached cells, and 50 nM CLX12 with 20 ng/ml of hFGF and hEGF in assays using neurosphere derived cells. Saracatinib was added at a concentration of 0.5 μM, 1 μM and 2.5 μM in the bottom well for all Saracatinib migration experiments. To quantify migrating cells, the transwell was removed and the top of the membrane was cleaned carefully with a cotton applicator to remove any remaining cells. All cells that had migrated through the Transwell membrane were lysed by adding 200 ul of CellTiter-Glo® Luminescent reagent and incubated for 10 minutes at room temperature. A standard curve was set up for each experiment. The percentage of cells that migrated through the Transwell membrane was determined by luminescence using the Veritas™ Microplate Luminometer (Turner Biosystems, Inc). The amount of migrating cells was normalized against the total cells seeded in a control well at the same time.

Generation of stable cell lines with Fyn knockdown. NP and NPA neurospheres were used to generate stable cell lines with Fyn knockdown. The pLenti pLKO-non-target shRNA control vector (SHC002) and two different pLenti-mouse shRNA vectors for Fyn were selected from Sigma Aldrich MISSION® shRNA Vectors. The Fyn shRNA identification numbers are: TRCN0000023383 (shFyn #1) and TRCN0000361213 (shFyn #2). The Fyn-shRNA lentivirus generation was performed by the Vector Core of the University of Michigan. Cells were infected

457 with the lentivirus as described previously by us [4]. After 48 hours, cells were selected with
458 puromycin at a concentration of 0.5 µg/µl. Immunoblotting was used to confirm Fyn knockdown.
459 Fyn shRNA #1 and #2 cells were used for *in vitro* experiments, and shFyn #2 cells were selected
460 for *in vivo* experiments.
461
462 **Intracranial implantable syngeneic mouse glioma model.** All animal studies were conducted
463 according to the guidelines approved by the Institutional Animal Care and Use Committee
464 (IACUC) at the University of Michigan. Intracranial surgeries were performed according to the
465 approved IACUC protocol, PRO00007666 for C57BL/6 immune-competent mice and
466 PRO00007669 for NSG immune-suppressive mice. Glioblastoma tumors were generated by
467 intracranial implantation of 3.0 x 10^4 neurosphere cells into the striatum of mouse brains.
468 Neurosphere cells were originated from the Sleeping beauty model[2,48]. Detailed methodology is
469 described in Supplementary Information.
470
471 **Genetically engineered mouse glioma model (GEMM) generation for Fyn Knockdown.** The
472 animal model study was conducted in C57BL/6 strain (Jackson Laboratory, Bar Harbor ME,
473 000664). according to guidelines approved by the Institutional Animal Care and Use Committee
474 at the University of Michigan and the approved IACUC protocol PRO00007617.
475 A Fyn knockdown glioma murine model and the appropriate comparisons/controls were created
476 by the Sleeping Beauty (SB) transposon system. This system is used to integrate genetic lesions
477 into the genomic DNA of neonatal mice. Female and male postnatal day 1 (P01) wild-type
478 C57BL/6 mice were used in all experiments [2]. The genotype of SB generated tumors involved
479 these combinations: (i) shp53 and NRAS **(NP)**, (ii) shp53, NRAS and shFyn **(NPF)**, (iii) shp53,
480 NRAS and shATRX **(NPA)**, (iv) shp53, NRAS, shATRX and shFyn **(NPAF)**, (v) shp53, NRAS and
481 PDGFβ **(NPD)**, (vi) shp53, NRAS, PDGFβ and shFyn **(NPDF)**. Mice were injected according to a
482 protocol previously described by our lab [20]. Tumors then develop intracranially *de novo* from

neural progenitor cells. To design and cloning of the shRNA targeting the FYN gene (pT2-shFyn-GFP4), we tested two 22 base pair sequences in a 97 base pair hairpin sequence for the mouse Fyn gene (shFyn-(1): HP_106460 and shFyn-(2): HP_292369) selected from candidate sequences within the RNAi codex database (http://cancan.cshl.edu/cgi-bin/Codex/Codex.cgi).

Immunoblotting. Glioma cells (1.0 x 10^6 cells) were seeded in a 100 mm dish and grown for various times according to each experimental design. Detailed protocol is shown in supplementary information.

Immunohistochemistry of paraffin embedded brains (IHC-DAB). Immunohistochemistry assay was performed in 4% paraformaldehyde fixed and paraffin embedded tissue in section of 5µm as described previously by our laboratory [49]. Immunohistochemistry protocol was modified from a protocol used in our laboratory [20] as described in Supplementary Information.

Immunofluorescence of paraffin embedded brains. Brains fixed in 4% paraformaldehyde were then processed and embedded in paraffin and sectioned as described previously by our laboratory [49]. Fyn antibody was then detected with Alexa Fluor™ 488 Tyramide SuperBoost™ Kit - Goat anti-Rabbit IgG (Cat. No. B40922) Tyramide SuperBoost™ following the manufacture instructions (Invitrogen- Thermo Fisher Scientific).

RNA isolation and RNA-Sequencing. Three tumors of each experimental group NP vs. NPF were studied by RNA-Seq analysis. RNA was isolated using the RNeasy Plus Mini Kit (© QIAGEN) following the manufacture instructions. RNA-sequencing was performed at the University of Michigan DNA Sequencing Core.

RNA-Seq libraries were constructed with the TruSeq Stranded Total RNA Library Prep kit (Illumina, San Diego, CA) and validated for control by TapeStation and qPCR using Kapa's library quantification kit for Illumina Sequencing platforms (Kapa Biosystems,Wilmington MA).
The samples were pooled, clustered on an Illumina cBot and sequenced on the Illumina HiSeq 4000, as paired-end 50 nt reads, according to manufacturer's recommended protocols. Detailed protocol is described in Supplementary information.

RNA-Sequencing data analysis. Tuxedo Suite software package was used for alignment, differential expression analysis, and post-analysis diagnostics [50-52] by the University of Michigan Bioinformatics Core as described in detail in SI Appendix.. Volcano plots analysis for DE genes were produced with the R base package in our lab. Differentially expressed genes of NPF versus NP tumors were used for Gene set enrichment analysis (GSEA). Network analysis was performed using Cytoscape and Reactome App to analyze the interaction of the differentially expressed genes. Detailed bioinformatics analysis is described in Supplementary Information.

Statistical Analysis. All *in vivo* experiments were performed in at least three or more independent biological replicates, depending on the specific analysis. Data is presented as the mean ± SEM. The difference was considered statistically significant when $p < 0.05$ using the ANOVA test to compare two or more samples. In experiments that included one variable, the one-way ANOVA test was used. In experiments with two independent variables, the two-way ANOVA test was employed. A posterior Tukey's multiple comparisons test was used for mean comparisons. Student t-test was used to compare unpaired data from two samples. Survival data were entered into Kaplan-Meier survival curves plots, and statistical analysis was performed using the Mantel log-rank test. The effect size is expressed in median survival (MS). Linear mixed effects models were used to compare Fyn levels between tumor groups determined by immunofluorescence imaging. Linear mixed effects models were also used to compare the P-H3-

S10 quantification by immunohistochemistry in tumor groups. This model considers that multiple observations per animal are correlated through a random effect. Significance was determined if $p<0.05$. All analyses were conducted using GraphPad Prism (version 6.01), SAS (version 9.4, SAS Institute, Cary, NC) or Infostat (Version 2014, National University of Cordoba, Argentina). The statistical tests used are indicated within the figure legends.

References

1 Reifenberger, G., Wirsching, H. G., Knobbe-Thomsen, C. B. & Weller, M. Advances in the molecular genetics of gliomas - implications for classification and therapy. *Nature reviews. Clinical oncology* **14**, 434-452, doi:10.1038/nrclinonc.2016.204 (2017).

2 Koschmann, C. *et al.* ATRX loss promotes tumor growth and impairs nonhomologous end joining DNA repair in glioma. *Sci Transl Med* **8**, 328ra328, doi:10.1126/scitranslmed.aac8228 (2016).

3 Frattini, V. *et al.* The integrated landscape of driver genomic alterations in glioblastoma. *Nature genetics* **45**, 1141-1149, doi:10.1038/ng.2734 (2013).

4 Preusser, M., Lim, M., Hafler, D. A., Reardon, D. A. & Sampson, J. H. Prospects of immune checkpoint modulators in the treatment of glioblastoma. *Nature reviews. Neurology* **11**, 504-514, doi:10.1038/nrneurol.2015.139 (2015).

5 Ratnam, N. M., Gilbert, M. R. & Giles, A. J. Immunotherapy in CNS cancers: the role of immune cell trafficking. *Neuro-oncology* **21**, 37-46, doi:10.1093/neuonc/noy084 (2019).

6 Thomas, S. M. & Brugge, J. S. Cellular functions regulated by Src family kinases. *Annual review of cell and developmental biology* **13**, 513-609, doi:10.1146/annurev.cellbio.13.1.513 (1997).

7 Palacios, E. H. & Weiss, A. Function of the Src-family kinases, Lck and Fyn, in T-cell development and activation. *Oncogene* **23**, 7990-8000, doi:10.1038/sj.onc.1208074 (2004).

8 Senis, Y. A., Mazharian, A. & Mori, J. Src family kinases: at the forefront of platelet activation. *Blood* **124**, 2013-2024, doi:10.1182/blood-2014-01-453134 (2014).

9 Zhang, S. *et al.* Suppression of protein tyrosine phosphatase N23 predisposes to breast tumorigenesis via activation of FYN kinase. *Genes Dev* **31**, 1939-1957, doi:10.1101/gad.304261.117 (2017).

10 Maksumova, L. *et al.* Protein tyrosine phosphatase alpha regulates Fyn activity and Cbp/PAG phosphorylation in thymocyte lipid rafts. *J Immunol* **175**, 7947-7956 (2005).

11 Yamauchi, J. *et al.* Phosphorylation of cytohesin-1 by Fyn is required for initiation of myelination and the extent of myelination during development. *Science signaling* **5**, ra69, doi:10.1126/scisignal.2002802 (2012).

12 Lu, K. V. *et al.* Fyn and SRC are effectors of oncogenic epidermal growth factor receptor signaling in glioblastoma patients. *Cancer research* **69**, 6889-6898, doi:10.1158/0008-5472.can-09-0347 (2009).

13 Yadav, V. & Denning, M. F. Fyn is induced by Ras/PI3K/Akt signaling and is required for enhanced invasion/migration. *Molecular carcinogenesis* **50**, 346-352, doi:10.1002/mc.20716 (2011).

14 Jensen, A. R. *et al.* Fyn is downstream of the HGF/MET signaling axis and affects cellular shape and tropism in PC3 cells. *Clinical cancer research : an official journal of the American Association for Cancer Research* **17**, 3112-3122, doi:10.1158/1078-0432.ccr-10-1264 (2011).

15 Lewis-Tuffin, L. J. *et al.* Src family kinases differentially influence glioma growth and motility. *Mol Oncol* **9**, 1783-1798, doi:10.1016/j.molonc.2015.06.001 (2015).

16 Han, X. *et al.* The role of Src family kinases in growth and migration of glioma stem cells. *Int J Oncol* **45**, 302-310, doi:10.3892/ijo.2014.2432 (2014).

17 Yamaguchi, H. *et al.* Saracatinib impairs the peritoneal dissemination of diffuse-type gastric carcinoma cells resistant to Met and fibroblast growth factor receptor inhibitors. *Cancer Sci* **105**, 528-536, doi:10.1111/cas.12387 (2014).

18 Liu, K. J. *et al.* Saracatinib (AZD0530) is a potent modulator of ABCB1-mediated multidrug resistance in vitro and in vivo. *Int J Cancer* **132**, 224-235, doi:10.1002/ijc.27649 (2013).

19 Cavalloni, G. *et al.* Antitumor activity of Src inhibitor saracatinib (AZD-0530) in preclinical models of biliary tract carcinomas. *Mol Cancer Ther* **11**, 1528-1538, doi:10.1158/1535-7163.mct-11-1020 (2012).

20 Núñez, F. J. *et al.* IDH1-R132H acts as a tumor suppressor in glioma via epigenetic up-regulation of the DNA damage response. **11**, eaaq1427, doi:10.1126/scitranslmed.aaq1427 %J Science Translational Medicine (2019).

21 Wilson, T. J., Zamler, D. B., Doherty, R., Castro, M. G. & Lowenstein, P. R. Reversibility of glioma stem cells' phenotypes explains their complex in vitro and in vivo behavior: Discovery of a novel neurosphere-specific enzyme, cGMP-dependent protein kinase 1, using the genomic landscape of human glioma stem cells as a discovery tool. *Oncotarget* **7**, 63020-63041, doi:10.18632/oncotarget.11589 (2016).

22 Elias, D. & Ditzel, H. J. Fyn is an important molecule in cancer pathogenesis and drug resistance. *Pharmacol Res* **100**, 250-254, doi:10.1016/j.phrs.2015.08.010 (2015).

23 Zheng, J., Li, H., Xu, D. & Zhu, H. Upregulation of Tyrosine Kinase FYN in Human Thyroid Carcinoma: Role in Modulating Tumor Cell Proliferation, Invasion, and Migration. *Cancer Biother Radiopharm* **32**, 320-326, doi:10.1089/cbr.2017.2218 (2017).

24 Vivier, E., Nunes, J. A. & Vely, F. Natural killer cell signaling pathways. *Science (New York, N.Y.)* **306**, 1517-1519, doi:10.1126/science.1103478 (2004).

25 Abram, C. L. & Lowell, C. A. The diverse functions of Src family kinases in macrophages. *Frontiers in bioscience : a journal and virtual library* **13**, 4426-4450 (2008).

26 Sugie, K., Jeon, M. S. & Grey, H. M. Activation of naive CD4 T cells by anti-CD3 reveals an important role for Fyn in Lck-mediated signaling. *Proceedings of the National Academy of Sciences of the United States of America* **101**, 14859-14864, doi:10.1073/pnas.0406168101 (2004).

27 Comprehensive genomic characterization defines human glioblastoma genes and core pathways. *Nature* **455**, 1061-1068, doi:10.1038/nature07385 (2008).

28 Brennan, C. W. *et al.* The somatic genomic landscape of glioblastoma. *Cell* **155**, 462-477, doi:10.1016/j.cell.2013.09.034 (2013).

29 Ceccarelli, M. *et al.* Molecular Profiling Reveals Biologically Discrete Subsets and Pathways of Progression in Diffuse Glioma. *Cell* **164**, 550-563, doi:10.1016/j.cell.2015.12.028 (2016).

30 Bowman, R. L., Wang, Q., Carro, A., Verhaak, R. G. & Squatrito, M. GlioVis data portal for visualization and analysis of brain tumor expression datasets. *Neuro-oncology* **19**, 139-141, doi:10.1093/neuonc/now247 (2017).

31 Saito, Y. D., Jensen, A. R., Salgia, R. & Posadas, E. M. Fyn: a novel molecular target in cancer. *Cancer* **116**, 1629-1637, doi:10.1002/cncr.24879 (2010).

32 Schenone, S. *et al.* Fyn kinase in brain diseases and cancer: the search for inhibitors. *Current medicinal chemistry* **18**, 2921-2942 (2011).

33 Jelic, D. *et al.* Homology modeling of human Fyn kinase structure: discovery of rosmarinic acid as a new Fyn kinase inhibitor and in silico study of its possible binding modes. *Journal of medicinal chemistry* **50**, 1090-1100, doi:10.1021/jm0607202 (2007).

34 Zhang, S. *et al.* Fyn-phosphorylated PIKE-A binds and inhibits AMPK signaling, blocking its tumor suppressive activity. *Cell Death Differ* **23**, 52-63, doi:10.1038/cdd.2015.66 (2016).

35 Gao, J. *et al.* Integrative analysis of complex cancer genomics and clinical profiles using the cBioPortal. *Science signaling* **6**, pl1, doi:10.1126/scisignal.2004088 (2013).

36 Cerami, E. *et al.* The cBio cancer genomics portal: an open platform for exploring multidimensional cancer genomics data. *Cancer discovery* **2**, 401-404, doi:10.1158/2159-8290.Cd-12-0095 (2012).

37 Schindler, C., Shuai, K., Prezioso, V. R. & Darnell, J. E., Jr. Interferon-dependent tyrosine phosphorylation of a latent cytoplasmic transcription factor. *Science (New York, N.Y.)* **257**, 809-813 (1992).

38 Au-Yeung, N., Mandhana, R. & Horvath, C. M. Transcriptional regulation by STAT1 and STAT2 in the interferon JAK-STAT pathway. *Jak-stat* **2**, e23931, doi:10.4161/jkst.23931 (2013).

39 Avalle, L., Pensa, S., Regis, G., Novelli, F. & Poli, V. STAT1 and STAT3 in tumorigenesis: A matter of balance. *Jak-stat* **1**, 65-72, doi:10.4161/jkst.20045 (2012).

40 Kim, H. S. & Lee, M. S. STAT1 as a key modulator of cell death. *Cellular signalling* **19**, 454-465, doi:10.1016/j.cellsig.2006.09.003 (2007).

41 Majoros, A. *et al.* Canonical and Non-Canonical Aspects of JAK-STAT Signaling: Lessons from Interferons for Cytokine Responses. *Frontiers in immunology* **8**, 29, doi:10.3389/fimmu.2017.00029 (2017).

42 Ivashkiv, L. B. IFNgamma: signalling, epigenetics and roles in immunity, metabolism, disease and cancer immunotherapy. *Nature reviews. Immunology* **18**, 545-558, doi:10.1038/s41577-018-0029-z (2018).

43 Simpson, J. A. *et al.* Intratumoral T cell infiltration, MHC class I and STAT1 as biomarkers of good prognosis in colorectal cancer. *Gut* **59**, 926-933, doi:10.1136/gut.2009.194472 (2010).

44 Leibowitz, M. S., Andrade Filho, P. A., Ferrone, S. & Ferris, R. L. Deficiency of activated STAT1 in head and neck cancer cells mediates TAP1-dependent escape from cytotoxic T lymphocytes. *Cancer immunology, immunotherapy : CII* **60**, 525-535, doi:10.1007/s00262-010-0961-7 (2011).

45 Qiu, L. *et al.* Expression patterns of NLRC5 and key genes in the STAT1 pathway following infection with Salmonella pullorum. *Gene* **597**, 23-29, doi:10.1016/j.gene.2016.10.026 (2017).

46 Kamran, N. *et al.* Current state and future prospects of immunotherapy for glioma. *Immunotherapy* **10**, 317-339, doi:10.2217/imt-2017-0122 (2018).

47 Wiesner, S. M. *et al.* De novo induction of genetically engineered brain tumors in mice using plasmid DNA. *Cancer research* **69**, 431-439, doi:10.1158/0008-5472.Can-08-1800 (2009).

48 Calinescu, A. A. *et al.* Transposon mediated integration of plasmid DNA into the subventricular zone of neonatal mice to generate novel models of glioblastoma. *Journal of visualized experiments : JoVE*, doi:10.3791/52443 (2015).

49 Calinescu, A. A. *et al.* Survival and Proliferation of Neural Progenitor-Derived Glioblastomas Under Hypoxic Stress is Controlled by a CXCL12/CXCR4 Autocrine-Positive Feedback Mechanism. *Clinical cancer research : an official journal of the*

American Association for Cancer Research **23**, 1250-1262, doi:10.1158/1078-0432.Ccr-15-2888 (2017).

50 Langmead, B., Trapnell, C., Pop, M. & Salzberg, S. L. Ultrafast and memory-efficient alignment of short DNA sequences to the human genome. *Genome biology* **10**, R25, doi:10.1186/gb-2009-10-3-r25 (2009).

51 Trapnell, C. *et al.* Differential analysis of gene regulation at transcript resolution with RNA-seq. *Nature biotechnology* **31**, 46-53, doi:10.1038/nbt.2450 (2013).

52 Trapnell, C., Pachter, L. & Salzberg, S. L. TopHat: discovering splice junctions with RNA-Seq. *Bioinformatics (Oxford, England)* **25**, 1105-1111, doi:10.1093/bioinformatics/btp120 (2009).

Acknowledgments

Work was supported by NIH/NINDS Grants: R37-NS094804, R01-NS105556 to M.G.C.; NIH/NINDS Grants R01-NS076991, and R01-NS096756 to P.R.L.; NIH/NIBIB: R01-EB022563; NIH/NCI U01CA224160; the Department of Neurosurgery and Leah's Happy Hearts to M.G.C. and P.R.L. A.C. was funded in part by University of Michigan, MICHR Postdoctoral Translational Scholars Program, TL1 TR002240-02, Project F049768.

Author contributions

A.C and PRL conducted and designed the study. A.C and PRL prepared the manuscript with support of the following authors M.G.C, P.J.D and PK. A.C, P.J.D, A.E.A, P.K, M.V, D.B.Z, P.P, F.J.N performed the experiments and acquired the data. A.C, P.J.D and M.V analyzed and interpreted the data. L.Z performed the statistical analysis. P.R.L. and M.G.C. directed the research and generated the funding. All authors read and edited the manuscript.

Competing interests

All authors of this paper declare no competing interests.

Fig. 1

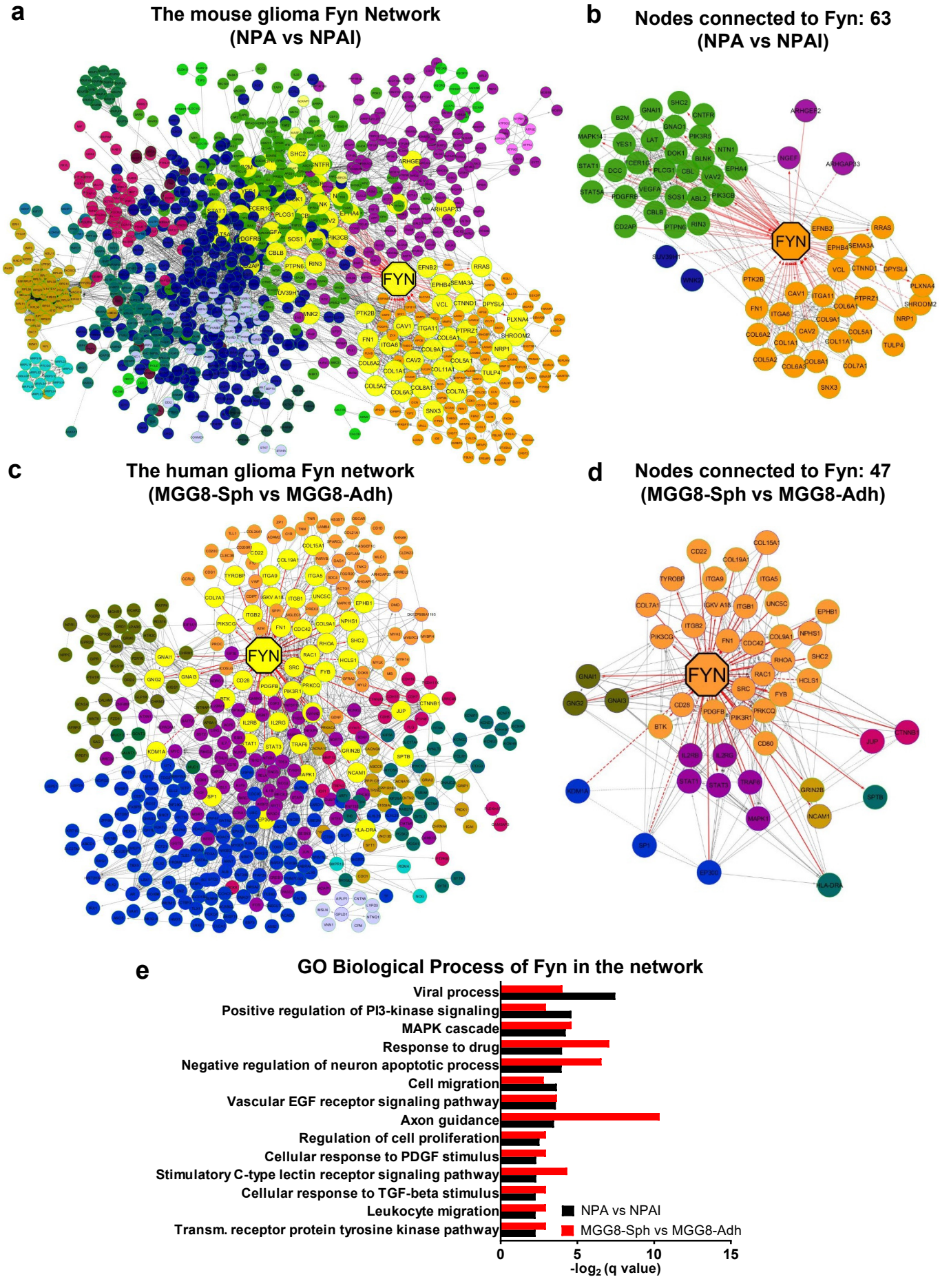

Fig. 1: Differential gene expression and network analysis identified Fyn as a key regulator of aggressiveness in rodent and human glioma stem cells.

a) Network maps of genes differentially expressed in either malignant NPA glioma stem cells, or in less malignant NPAI mouse glioma stem cells. Image displays entire network. Fyn protein kinase is shown as larger yellow octagonal node. Network was analyzed by the Reactome Functional Interaction (FI) application from Cytoscape. Cluster of nodes shown in the same color illustrate a module of highly interacting genes in the network, which also share functional characteristics. The Fyn subnetwork is highlighted in yellow. **b)** Right panel illustrates a higher magnification of the isolated mouse Fyn subnetwork. Fyn and its first neighbors are shown; red lines indicate the edges connecting nodes. Fyn is a highly connected node with a degree of 63 interactions in the network (4^{th} most connected node). The GO corresponding to this network are detailed in Supplementary Table 1a. Note GO related to growth factor and intracellular signaling. **c)** Network analysis of differentially expressed genes of more malignant MGG8-Spheres vs the less malignant MGG8-Adherent human glioma stem cells. Image displays entire network, where Fyn protein kinase is depicted as a larger octagonal node. **d**) This panel illustrates the isolated human Fyn subnetwork. Fyn and its first neighbors are shown; red lines indicate edges connecting nodes. Fyn tyrosine kinase is a highly connected node with a degree of 47 interactions in the network (7^{th} most connected node). The GO corresponding to this network are detailed in Supplementary Table 1c. Note GO related to growth factor and intracellular signaling. **e)** Functional enrichment analysis of the gene ontology (GO) terms of the network obtained from Figures 1a and 1b. The bar graph displays overrepresented GO Biological process that include Fyn tyrosine kinase. Groups represented are NPA vs NPAI (black bars) and MGG8-Spheres vs MGG8-Adherent cells (red bars). GO term significance was determined by a cutoff of q-value (FDR) < 0.2. GO terms were plotted against the -Log 2 of the q-value (FDR). Lower panels show the FI sub-network based on a set of genes that directly interact with Fyn inside its module.

Fig. 2

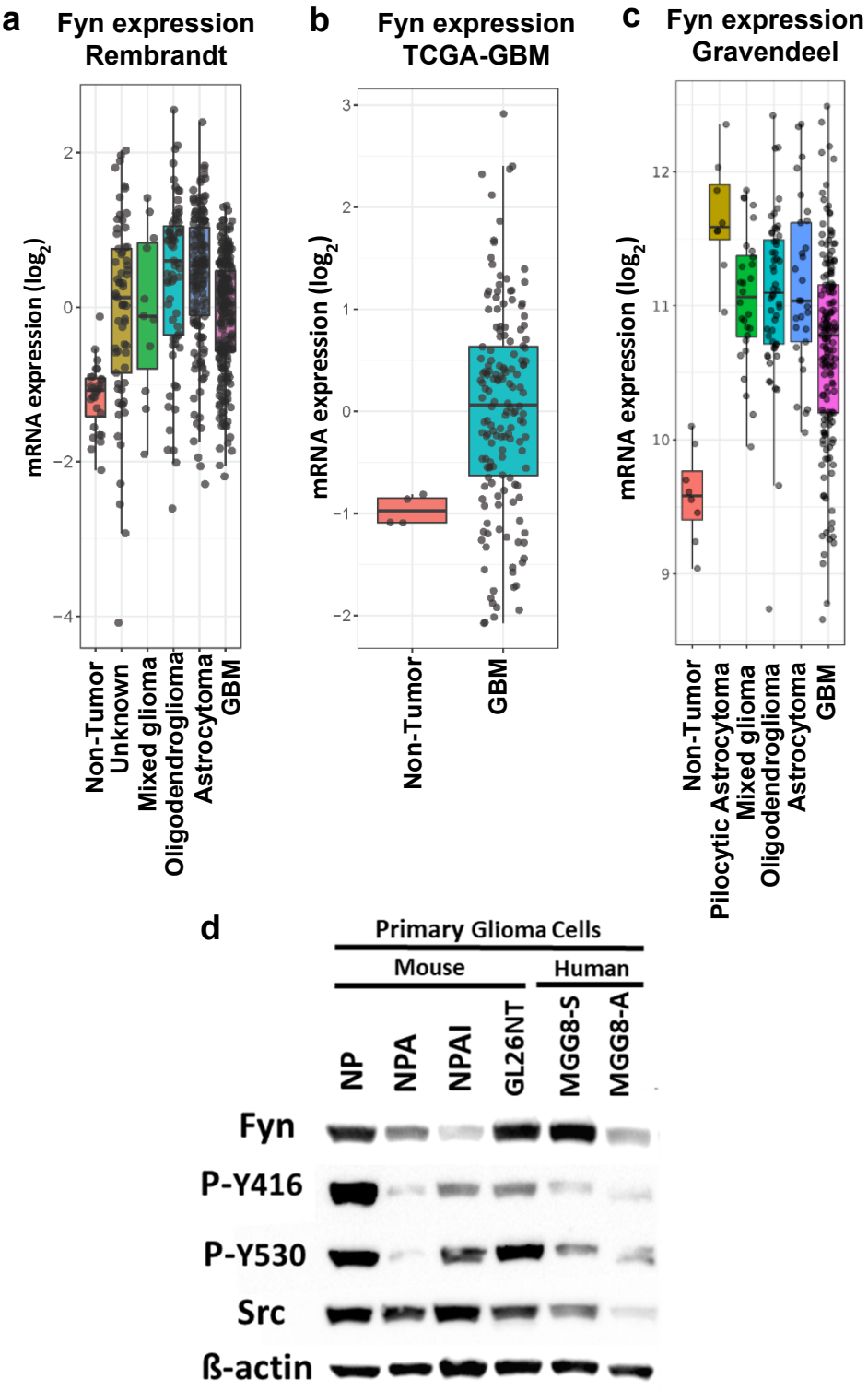

Fig. 2: Gene expression analysis of Fyn in human glioma tumors and mouse and human glioma cells shows a correlation with aggressiveness

a-b-c) mRNA expression analysis of Fyn in normal brain tissue vs different glioma subtype tissue from Rembrandt, TCGA and Gravendeel database. The data was obtained from the Gliovis (http://gliovis.bioinfo.cnio.es) database. **a)** Rembrandt dataset: mRNA expression of Fyn in non-tumor brain tissue vs glioma subtypes (Unknown, Mixed glioma, Oligodendroglioma, Astrocytoma and Glioblastoma). Graph shows the $\log_2$ mRNA expression levels of Fyn. Statistical significance was given within the corresponding databases (pairwise t-test with Bonferroni correction). Non Tumor-Unknown p-value= $1x10^{-6}$; Non Tumor-Mixed glioma p-value= $8x10^{-3}$; Non Tumor-Oligodendroglioma p-value= $1x10^{-12}$; Non Tumor-Astrocytoma p-value= $5x10^{-15}$; Non Tumor-GBM p-value= $4.3x10^{-8}$. **b)** TCGA data: Graph shows the Log2 mRNA expression levels of Fyn. Statistical significance was determined using the Pairwise t-test. p-value was determined by Bonferroni correction. Non Tumor-GBM p-value= 5.1E-02. **c)** Gravendeel database: Non Tumor-Pilocytic Astrocytoma p-value= 2.7E-08; Non Tumor-Mixed glioma p-value= 1.2E-06; Non Tumor-Oligodendroglioma p-value= 1.2E-7; Non Tumor-Astrocytoma p-value= 2.1E-7; Non Tumor-GBM p-value= 1.1E-04. **d)** Western blot (WB) analysis comparing Fyn levels in mouse (GL26, NP, NPA, NPAI) and human (MGG8-Sphere and MGG8-Adherent) glioma cells. WB also shows the expression levels of Src, P-Tyrosine-416 (phosphorylated form of the Src family kinase members at Tyr-416) and P-Tyrosine-530 (phosphorylated form of the Src family kinase members at Tyr-530). β-actin was used as loading control. Western Blot analysis demonstrates that Fyn levels positively correlate with glioma cell malignancy.

Fig. 3

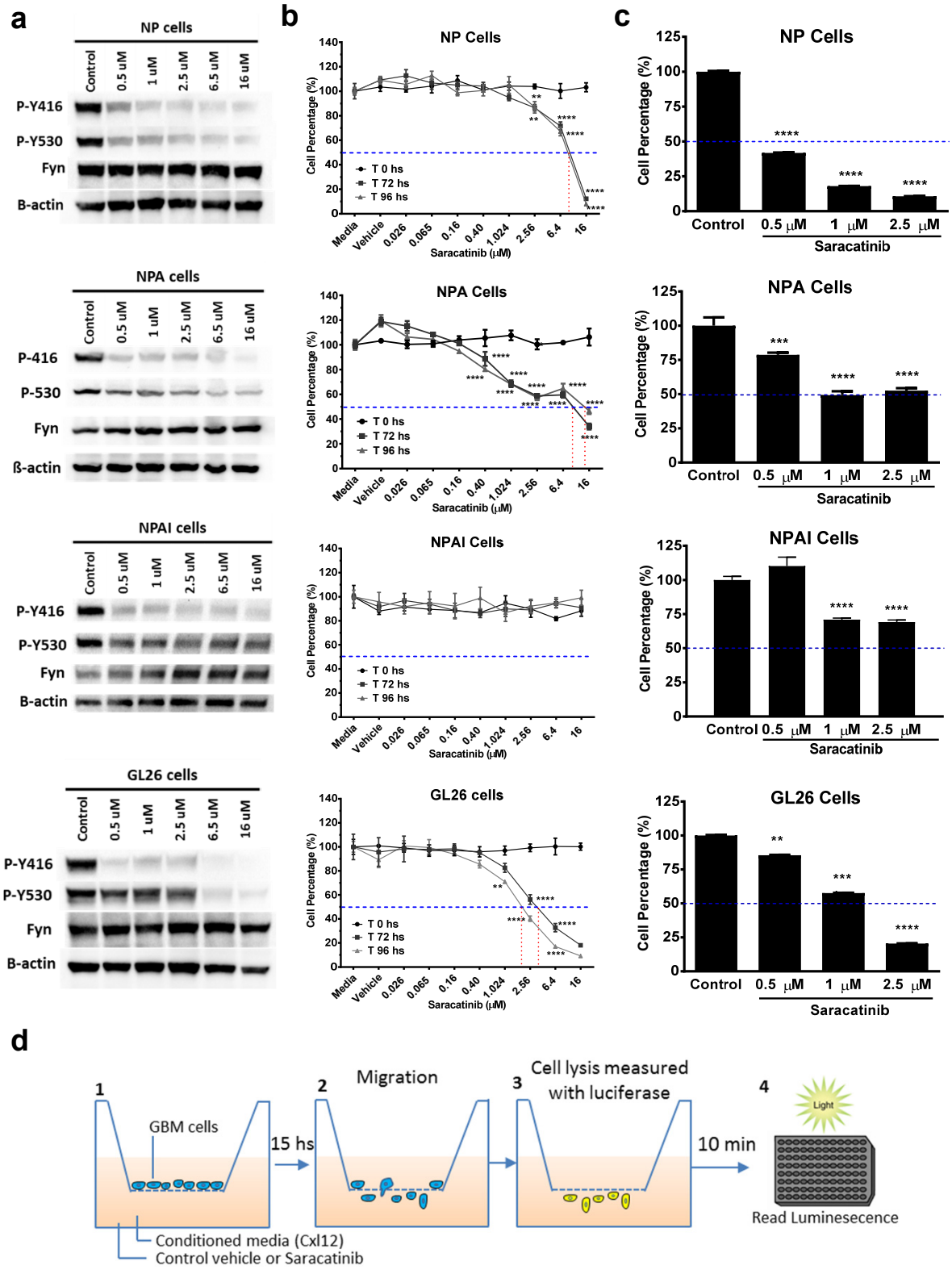

Fig. 3: Inhibition of Src family kinase activity by Saracatinib treatment decreases cell viability and migration of malignant glioma cells.

a) Western Blot (WB) analysis for P-Tyrosine-416, P-Tyrosine-530, Fyn and Src proteins was performed in mouse glioma cells (NP, NPA, NPAI and GL26) after 48 hours of treatment with the indicated doses of Saracatinib. β-actin was used as loading control. **b)** Cell viability assay performed on mouse glioma cells (NP, NPA, NPAI and GL26) in response to Saracatinib at the indicated doses. Cell viability was evaluated by CellTiterGlo assay performed at 0 hours, 72 hours and 96 hours post Saracatinib treatment. The results are expressed in percent cell viability relative to control, and the statistical significance was determined using two-way ANOVA test. *p<0.05, **p<0.01, ***p<0.001, ****p<0.0001. Error bars represent ±SEM. Experiment was performed 3 times with three replicates per treatment condition. Treatment with media alone and media plus ethanol drug vehicle were used as controls. **c)** Transwell Cell Migration assay was performed on mouse glioma cells (NP, NPA, NPAI and GL26) after 15 hours of treatment with Saracatinib at the indicated doses. Data is expressed as percentage of migrating cells relative to the control (ethanol vehicle). Error bars represent ±SEM. Experiment was performed 3 times with three replicates per treatment. Statistical significance was determined using One-way ANOVA test. ***p<0.001, ****p<0.0001. **d)** Schematic representation of the Transwell migration assay. GBM cells (blue) were seeded on the top of the Transwell and incubated for 15 hours in conditioned media with Cxl12 50 nM. The migrated cells were analyzed using CellTiter-Glo® to measure the viable cells.

Fig. 4

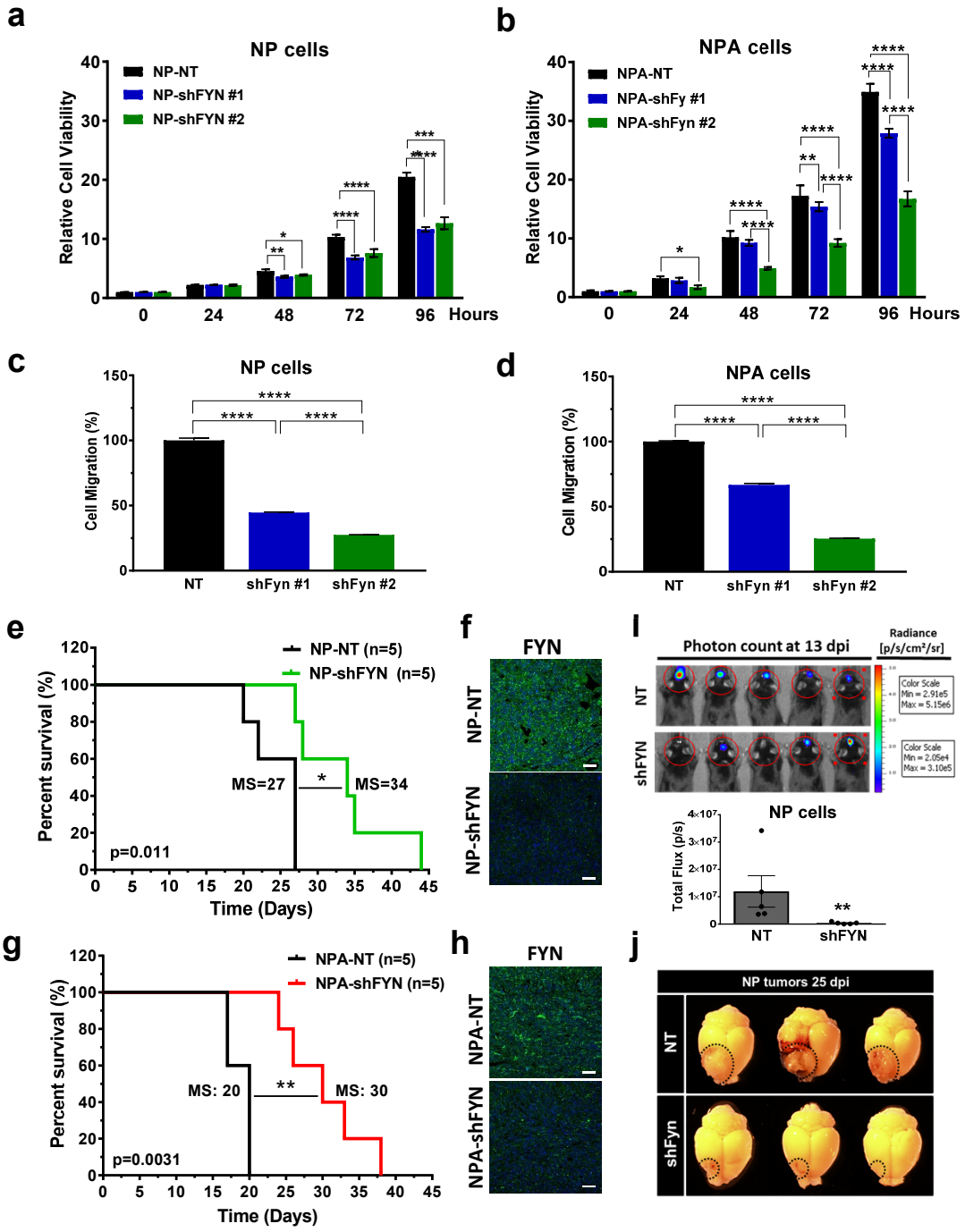

Fig. 4: Downregulation of Fyn reduces *in vitro* glioma stem cell proliferation and migration, and, *in vivo* increases median survival and reduces tumor growth.

a, b) Cell viability analysis in NP **(a)** and NPA **(b)** cells. Fyn downregulation reduced cell proliferation compared to control cells. Experiments were performed in triplicate. Two-way ANOVA test. *p < 0.05; **p < 0.01; ***p <0.001, ****p <0.0001. Error bars represent ±SEM. **c, d)** Cell migration analysis for NP **(c)** and NPA **(d)** cells. Fyn downregulation decreased cell migration compared to control cells. Three independent experiments were performed. One-way ANOVA test. ****p <0.0001 Error bars represent ±SEM. **e)** Kaplan–Meier survival curve of glioma generated by intracranial implantation. Mice bearing gliomas with Fyn knockdown displayed significant increases in median survival (MS). Five animals (n=5) were used per experimental condition. Log-rank (Mantel-Cox) test (*p=0.011). **f)** Fyn expression was detected by immunofluorescence (Alexa 488). Nuclei are labeled by DAPI; representative confocal images (20x, 1240 x 1240 pixels); scale bar: 50 μm. shFyn tumors showed decreased expression of Fyn compared to controls, in accordance with WB expression levels of the implanted cells. **g)** Kaplan–Meier survival curves. Mice bearing gliomas with Fyn knockdown displayed significant increase in MS compared to the control. Five animals (n=5) were used per experimental condition. Log-rank (Mantel-Cox) test (**p=0.0031). **h)** Fyn expression was detected by immunofluorescence (Alexa 488). Nuclei are labeled by DAPI. Representative confocal images (20x, 1240 x 1240 pixels). Scale bar: 50 μm. shFyn tumors showed decreased expression of Fyn compared to controls; in accordance with WB expression levels of the implanted cells. **i)** Animals harboring shFyn tumors showed a significant decrease in bioluminescence signal at 13 days post implantation (dpi). Luminescence intensity was measured using photons/s/cm2/sr and total flux (photon/s). Bar graph represents the luminescence intensity as (photon/s) in five (n=5) animals per group. Error bars represent ±SEM. Statistical significance was determined using a t-test. **p <0.01. **j)** Representative picture of the tumor size seen from the brain's surface analyzed at 25 dpi of animals harboring NP-NT vs NP-shFyn tumors. Tumors with Fyn downregulation displayed decreased tumor compared to the control.

Fig. 5

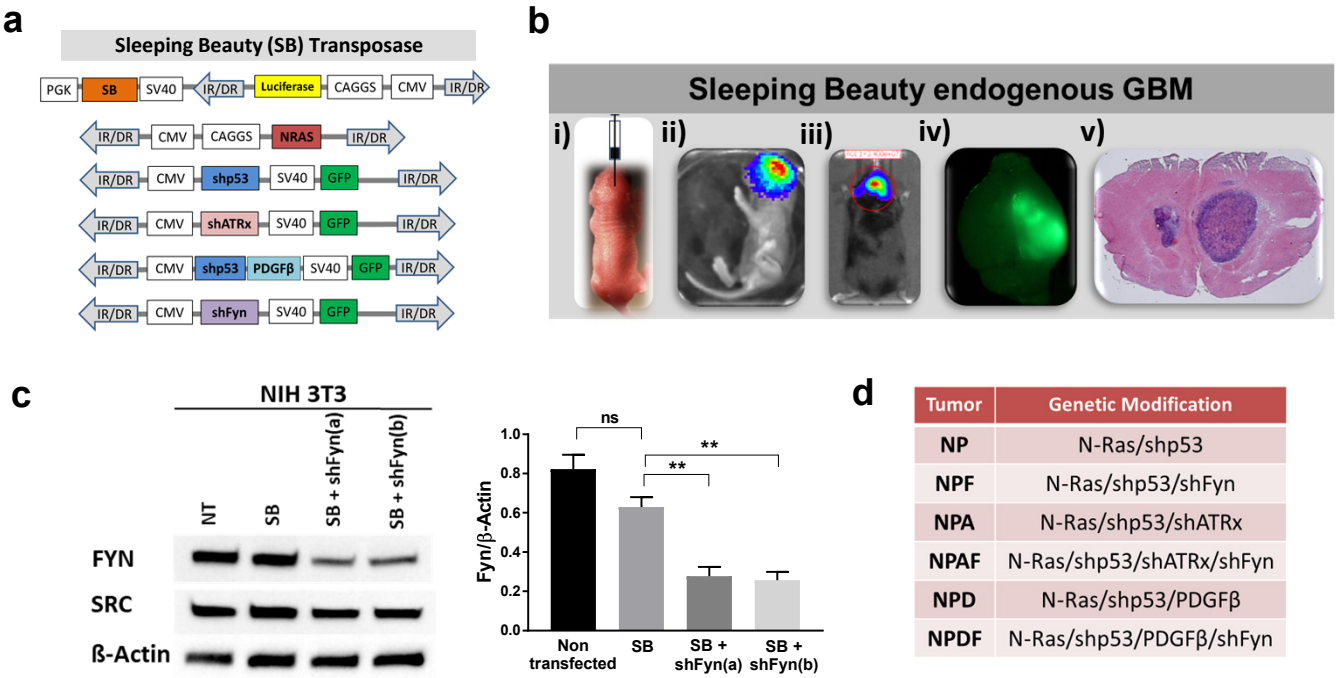

Tumor	Genetic Modification
NP	N-Ras/shp53
NPF	N-Ras/shp53/shFyn
NPA	N-Ras/shp53/shATRx
NPAF	N-Ras/shp53/shATRx/shFyn
NPD	N-Ras/shp53/PDGFβ
NPDF	N-Ras/shp53/PDGFβ/shFyn

Fig. 5: Genetically engineered mouse glioma models for Fyn downregulation

a) Schematic representation of the Sleeping Beauty Transposon System (SB) plasmids used to generate gliomas with Fyn downregulation. Plasmids include the following DNA sequences: Luciferase, NRAS-GV12, shATRX-GFP, shP53-GFP, shP53-PDGFβ-GFP and shFyn-GFP). **b)** Representative pictures showing tumor development in the SB genetically engineered mouse model: i) plasmid injection in P1 neonatal mice. ii) bioluminescence imaging of a neonatal mouse 1-day post injection (1 dpi) confirming the efficiency of transduction; iii) bioluminescence showing tumor development in an adult mouse harboring NP-shFyn glioma at 120 dpi; iv) fluorescence image of a mouse brain harboring a NP-shFyn glioma tumor co-expressing GFP at protocol end point; v) H&E staining of a NP-shFyn brain tumor sections at protocol end point. **c)** Western Blot (WB) analysis shows downregulation of Fyn levels. NIH-3T3 mouse cells transfected for 48 hours with the corresponding vectors. NT: Non-transfected cells, SB: cells transfected with the SB transposon vector. SB+shFyn: cells transfected with the SB transposon vector in addition to shFyn(a): HP_106460 or shFyn(b): HP_292369. WB shows that expression levels of Src were unchanged with transfection of the SB+shFyn vectors. β-actin was used as loading control. Bar graphs represent the quantitative analysis of the WB. Values were calculated by normalizing Fyn band density to the band density of β-actin. Quantification was performed using ImageJ software. WB quantifications performed in 3 independent experiments. Statistical significance was determined using One-way ANOVA test. **p < 0.01, ns: non-significance. Error bars represent ±SEM. **e)** Genotypes of the different SB tumors generated are indicated in the table.

Fig. 6

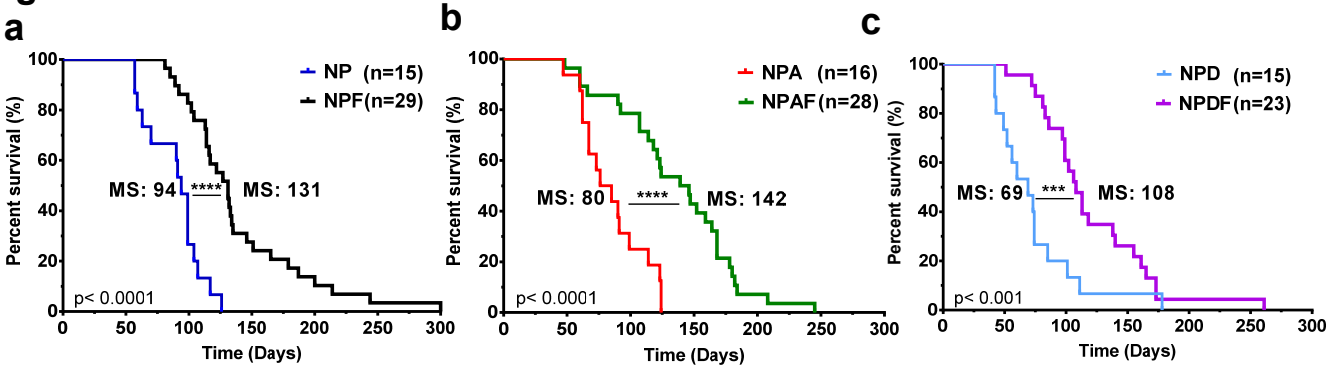

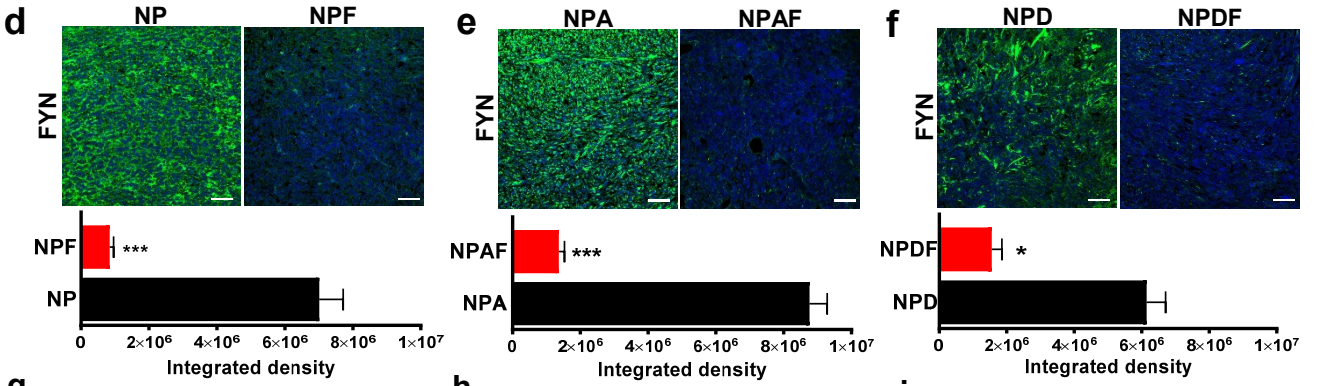

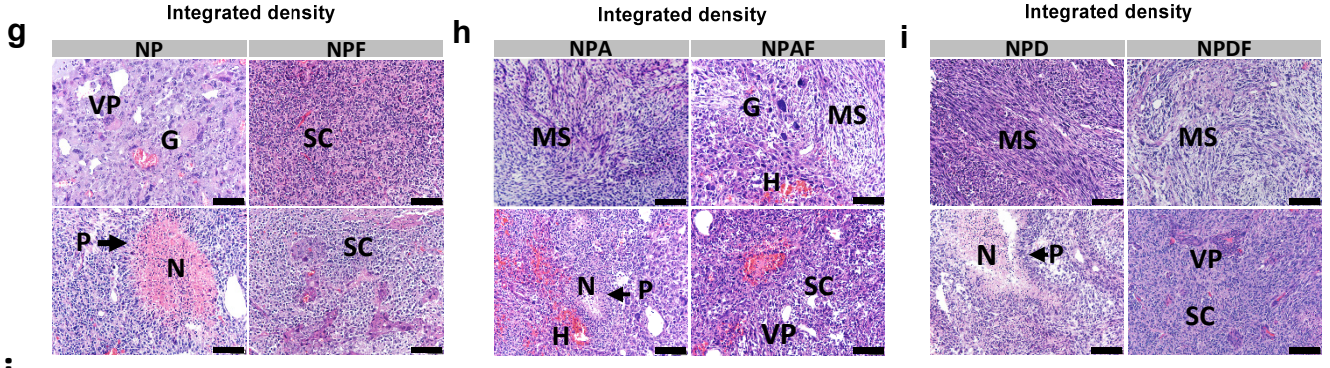

j

TUMOR	Giant cells	Necrosis	Hemorrhage	Small cells	Mesenchymal Sarcomatous components	Pseudo-Palisades	Vascular proliferation	Invasion
NP	++	++	+++	++	++	++	+++	+++
NPF	++	+++	+++	+++	+	+	+++	++
NPA	+++	+++	+++	++	+++	+/-	++	+++
NPAF	+++	+	+++	+++	++	+/-	++	+++
NPD	++	+++	+++	++	+++	+++	++	+++
NPDF	+	+	+	++	+++	++	++	+++

+/-	Very Low
+	Low
++	Medium
+++	High

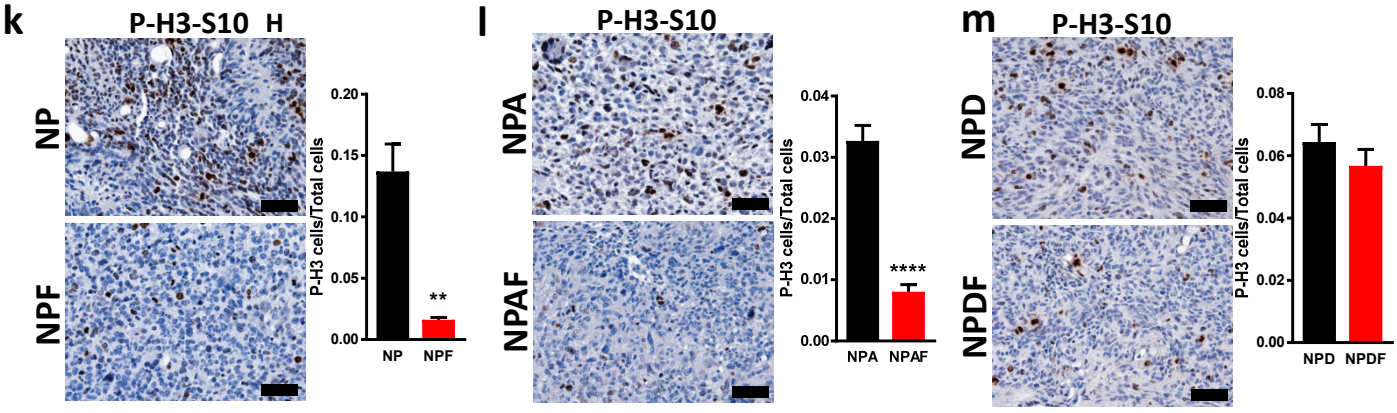

Fig. 6: *In vivo* studies: Fyn knockdown in genetically engineered mouse glioma models increases median survival and decreases tumor malignancy.

a, b, c) SB mouse glioma models demonstrate that animals bearing Fyn downregulation tumors exhibit a significant increase in median survival (MS). **(a)** Kaplan–Meier survival curve comparing NP (MS: 94 days; n: 15) versus NPF (MS: 131 days; n: 29). **(b)** Kaplan–Meier survival curve comparing NPA (MS: 80 days; n: 16) versus NPAF (MS: 142 days; n: 28). **(c)** Kaplan–Meier survival curve comparing NPD (MS: 69 days; n: 15) versus NPDF (MS: 108 days; n: 23). Log-rank (Mantel-Cox) test. *** p<0.001, ****p<0.0001. **d, e, f)** Analysis of Fyn expression in glioma tissues by immunofluorescence. Representative confocal images display Fyn expression in green (Alexa 488) and nuclei in blue (DAPI). Images (20x, 1240 x 1240 pixels). Scale bar: 50 μm. Bar graphs represent Fyn quantification in terms of fluorescence integrated density determined by Image-J. Five animals for each experimental condition were used for the analysis. Ten fields of each tumor section were selected at random. Error bars represent ±SEM. Linear mixed effects models. ***p<0.001, *p<0.05. **g, h, i)** Representative pictures of the histopathological analysis performed in tumor sections stained with H&E comparing the shFyn knockdown tumors with their respective controls. Magnification: 20x. Scale bars: 100 μm. Histopathological features. P: pseudo-palisades, N: necrosis, H: hemorrhage, VP: vascular proliferation, MS: mesenchymal sarcomatous components, SC: small cells, G: giant cells. **j)** Histopathological analysis. Glioma histopathological patterns of giant cells, necrosis, hemorrhage, small cells, mesenchymal sarcomatous component, pseudo-palisades and vascular proliferation were analyzed. Table represents the semi-quantitative analysis for the presence and abundance of markers: very low (+/-), low (+), Medium (++) and high (+++). **k, l, m)** Cell proliferation analysis in tumor sections performed by immunohistochemistry of P-H3-S10, which labels mitotically active cells. Positive P-H3-S10 cells were counted by Image-J software. Magnification: 40x. Scale bars: 50 μm. Bar graphs represent number of P-H3-S10 positive cells per total cells in the visual field. Five animals from each experimental condition were used. Ten fields of each section were selected at random. Error bars represent ±SEM. Linear mixed effects models. ***p<0.001, **p<0.01.

Fig. 7

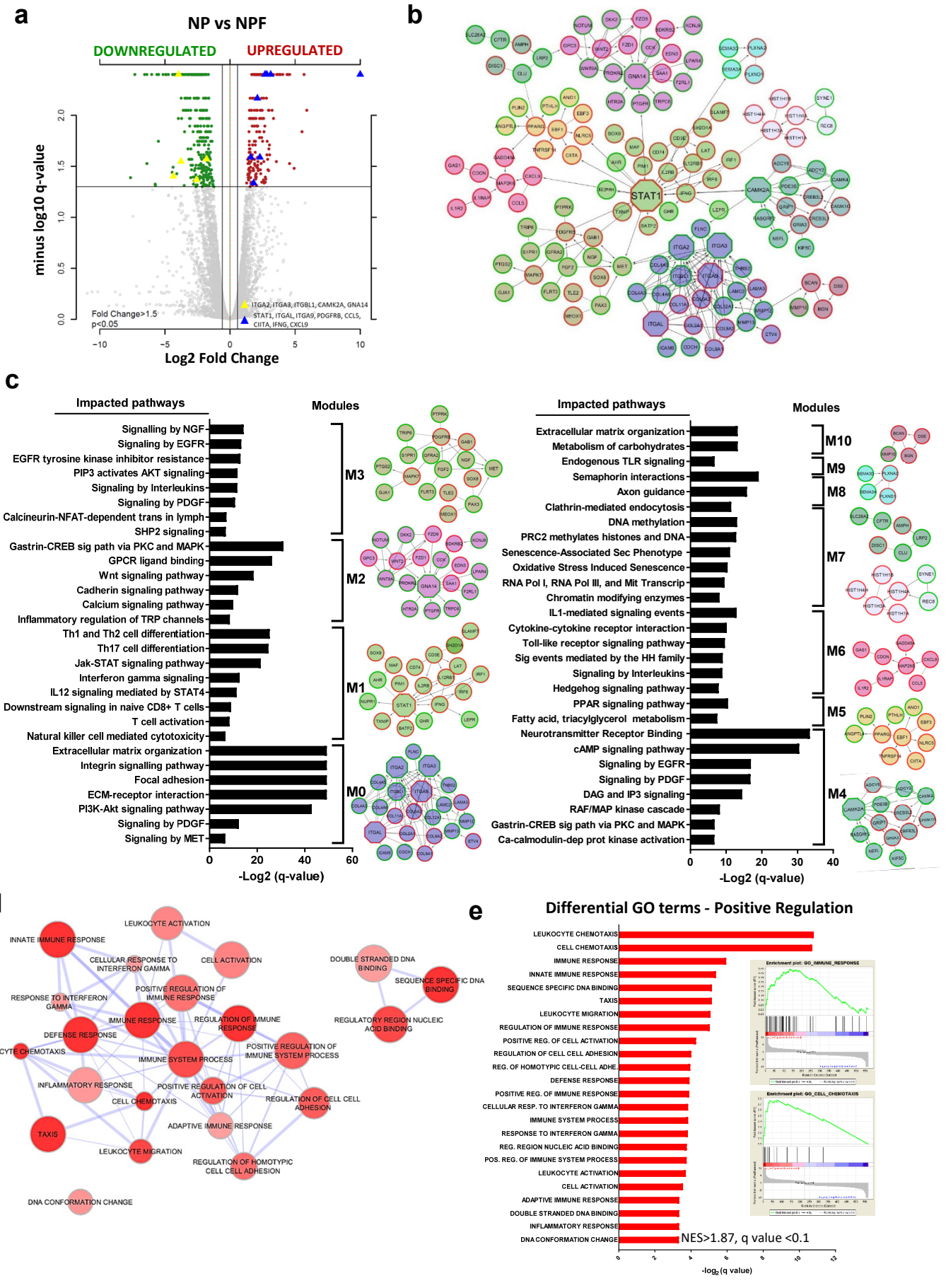

Fig. 7: Enrichment in immune-related pathways and gene ontologies suggest immune regulation as a mechanism of Fyn-mediated tumor growth control.

a) Volcano plot displays the DE genes from SB NPF vs SB NP mouse genetically engineered gliomas. Differentially expressed genes (n=567) were selected by fold change ≥ 1.5 and a q-value (FDR corrected p-value) < 0.05. Upregulated genes (n=226; red dots) and downregulated genes (n=341; green dots) are shown in A. Examples of genes that are upregulated (blue triangles) or downregulated (yellow triangles) are indicated in the lower right quadrant. The FDR-adjusted significance q-values were calculated using two-sided moderated Student's t-test. **b)** Network analysis of the DE genes comparing NPF versus NP mouse gliomas. Genes with a higher networks degree are highlighted with larger octagonal nodes. Clusters of nodes with the same color illustrate modules of highly interacting groups of genes in the network. Nodes with red border indicate upregulated genes and green borders indicate downregulated genes. **c)** Functional enrichment analysis of the pathways in each module of the network. Modules (nodes of the same color) represents a highly interacting group of genes in the network. The bar graph shows the overrepresented pathways plotted according to the minus Log2 FDR q-value (FDR). Pathways' selection cutoff was set at a q-value<0.01. **d)** Gene set enrichment analysis (GSEA) DE genes comparing NPF tumors versus NP tumors. Figure displays the enrichment map of the most significant upregulated GO terms (red nodes) in NPF gliomas at FDR<0.1 and p<0.05. No downregulated gene ontologies were significantly enriched at these statistical cutoffs. Node color indicates p-value; size indicates the frequency of the GO term in the GO database.

e) Functional enrichment analysis of overrepresented upregulated GO terms in NPF tumors compared with NP. The cutoff of the GO terms was drawn at a normalized enrichment score (NES) >1.87 and q-value<0.1. Enrichment plots of two of the most significant GO terms: "Immune response" (right hand side, top panel) and "Cell Chemotaxis" (right hand side, lower panel). These plots show the profile of the Running ES Score & Positions of GeneSet Members on the Rank Ordered List.

Fig. 8

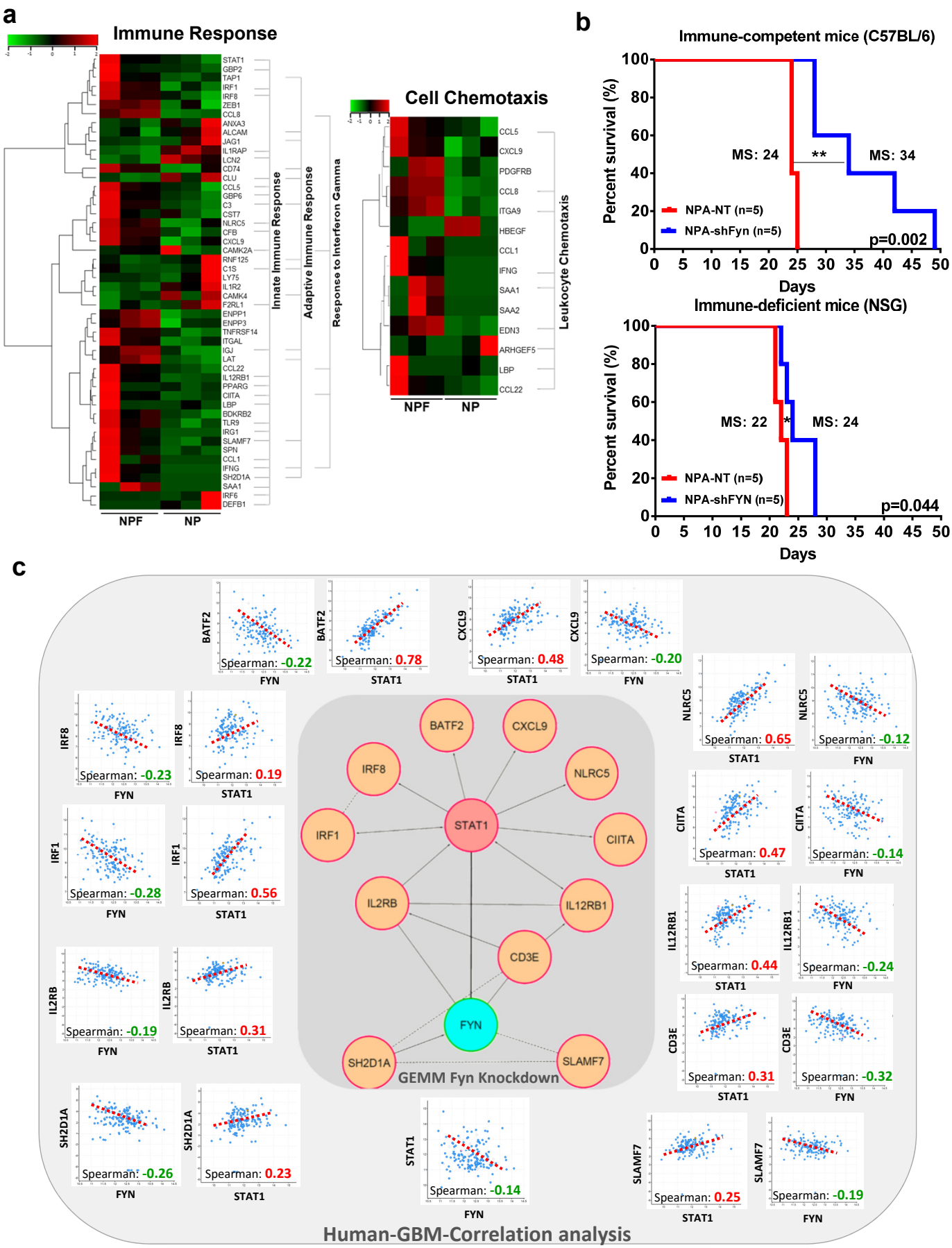

Fig. 8: Fyn downregulation increases immune responses: modulation of the STAT1 signaling pathway.

a) Heat maps illustrate gene expression pattern for Immune Response (left panel) and Cell Chemotaxis (right panel) GO terms in NPF vs. NP glioma tumors (3 biological replicates/group). Differentially upregulated genes are represented in red and downregulated genes are represented in green (q-value ≤ 0.05 and fold change ≥ ± 1.5). On the right hand side of the Immune Response heat map, brackets highlight DE genes that are present in upregulated immune GOs: “Innate Immune Response”, “Adaptive Immune Response”, and “Response to Interferon Gamma”. To the right of the Cell Chemotaxis heat map, a bracket highlights DE genes that are also present in significantly upregulated the GO “leukocyte chemotaxis”. **b)** Kaplan–Meier survival curve of glioma tumors generated by intracranial implantation of 3 x10^4 NPA-NT and NPA-shFyn cells into adult C57BL6 and NSG mice. Immune-competent C57BL6 mice bearing tumors with Fyn knockdown displayed a higher increase in median survival vs controls (MS: 24 vs 34 days; **p=0.002), while in immune-deficient mice the difference in survival was minor (MS: 22 vs 24 days; *p=0.044). For survival analysis, five animals (n=5) were used per experimental condition. Statistical analysis was determined by Log-rank (Mantel-Cox) test. **c)** Evaluation of the STAT1 signaling pathways using the gene expression and network analysis of the Fyn knockdown GEMM is shown in the central schematic. The correlations shown on the outside of this panel explore the relevance of the Fyn network in human samples of glioblastoma multiforme. We performed correlation analyses of FYN and STAT1 with DE genes identified from the Fyn network. Correlations of Fyn were opposite to those of STAT1. This indicates a similar inverse correlation to that encountered in mouse networks.